Energy Proceedings
Vol 45, 2024
ISSN 2004-2965

The influence of H_2S on plasma catalysis and the conversion of CH_4 and CO_2 in a dielectric barrier discharge reactor for biogas reforming into syngas

M. Umamaheswara Rao,[1] Harsh Jayesh Nagda,[1], Ch. Subrahmanyam[1]*

[1]Department of Chemistry, Indian Institute of Technology Hyderabad, Kandi, Sangareddy, Telangana, 502285, India

(*Corresponding author: csubbu@iith.ac.in)

ABSTRACT

Biogas is a type of sustainable energy produced by the anaerobic decomposition of organic matter derived from plants and animals. Biogas comprises significant quantities of CH_4, CO_2, and minor concentrations of H_2S. The substance is naturally introduced into the surrounding ecosystem, with its composition exhibiting variability contingent upon its origin. The biogas reforming process was conducted in a DBD-NTP reactor, using catalysts to enhance the total reaction efficiency under ambient circumstances. Fe/γ-Al_2O_3, Co/γ-Al_2O_3, and Ni/γ-Al_2O_3 catalysts were synthesized by the wet impregnation method and reduced the catalyst with H_2 gas in a tubular furnace. Synthesized catalysts were analyzed by XRD, BET, XPS and SEM. Prepared catalysts are integrated into a discharge zone of a DBD reactor and tested for biogas reforming reaction. The DBD plasma system produced an applied potential ranging from 16 kV to 22 kV, while maintaining a flow rate of 70 mL min^{-1} with a gas mixture contains CH_4, CO_2, and N_2 at a ratio of 30:30:10. The experiment started with performing the reaction in the absence of H_2S, followed by reaction with the addition of 0.054% H_2S (mixed with N_2), while ensuring a consistent residence duration. The data obtained from observations suggests that H_2S exerts a substantial influence on the process of conversion. When H_2S was added, the CH_4 conversion drastically decreased from 24% (without H_2S) to 15% (with H_2S), and the CO_2 conversion decreased from 21% to 17% at 22 kV with Ni/ γ-Al_2O_3 catalyst packed DBD. H_2S also has an impact on energy efficiency and syngas ratio. Moreover, H_2S has more impact on CH_4 than CO_2.

Keywords: Biogas reforming; Energy efficiency; Syngas production; DBD plasma

NOMENCLATURE

NTP	Non-Thermal Plasma
DBD	Dielectric Barrier Discharge
BET	Brunauer-Emmett-Teller
AC	Alternating Current
SEM	Scanning Electron Microscopy
FT	Fischer-Tropsch
IPC	In-Plasma Catalysis
CB	Carbon Balance

1. INTRODUCTION

The depletion of fossil fuels and the increasing apprehension regarding environmental consequences associated with energy conversion has prompted the exploration of novel approaches using renewable energy sources. Biogas is a sustainable energy source generated through the process of anaerobic digestion, which involves the decomposition of organic matter and animal manure. Based on the source, biogas has a composition of 25-50% CO_2, 35-75% CH_4, and traces of impurities like H_2S.[1,2] A variety of methodologies have been suggested for the generation of syngas, encompassing the gasification of diverse sources such as coal, municipal solid waste, and animal waste. The generation of syngas through non-thermal plasma technology is the subject of intensive study today.[3–5] The principal advantage of NTP is in its non-equilibrium characteristic, wherein the average electron energies range from 1 to 10 eV, while the temperature of the surrounding gas stays at ambient levels.[6] Excitation of atomic and molecular species, as well as the severing of chemical bonds, may be accomplished most effectively within this electron energy range by means of electron impact dissociation, excitation, and ionization.[7] Furthermore, the integration of non-thermal plasma and catalysts, known as plasma-catalysis, exhibits considerable promise in achieving synergistic effects.[8] This approach has the capability to reduce the required operating temperature

This is a paper for 15th International Conference on Applied Energy (ICAE2023), Dec. 3-7, 2023, Doha, Qatar.

of catalysts while simultaneously enhancing their catalytic activity and stability. Consequently, this leads to a substantial improvement in the conversion of reactants, yield and selectivity of desired products, as well as the overall energy efficiency of the process. Several non-thermal plasma sources have been utilized in biogas reforming, including dielectric barrier discharges (DBDs),[9] corona discharge,[10] and gliding arc discharge.[11] DBD has attracted growing attention as a viable method for synthesizing fuels and chemicals at low temperatures. Moreover, DBD produces a uniform discharge over the discharge volume. This is primarily due to its straightforward design and ability to be scaled up for industrial applications.

Despite extensive research on plasma-enhanced catalytic biogas reforming for syngas production, there is still a limited understanding of how to design highly efficient catalysts for this reaction. The study conducted by Kalai et al.[12] focused on the examination of biogas reforming using catalysts derived from Ni-Mg-Al hydrotalcite with Ce as promoter. The researchers emphasized that an increased Ce/Ni ratio resulted in improved stability and performance of the catalysts. Wang et al. observed that the addition of CeO_2 promoter had a positive impact on the process of plasma-catalytic biogas reforming. Nevertheless, the excessive doping of Ce led to a decrease in the quantity of active sites, accompanied by a reduction in the specific surface area. Consequently, this led to a decrease in the catalytic performance.[13]

The study conducted by Lucredio et al. aimed to examine the impact of incorporating La into a Ni-Rh/Al_2O_3 catalyst during the reforming process of a simulated sulfur-free biogas. The researchers observed that the presence of La resulted in a reduction of carbon deposition. This reduction was attributed to the promotion of gasification of carbon species.[14]

Moreover, many studies have been performed for biogas reforming reaction with model gas mixture without H_2S. The primary focus of this research is to investigate the effect of H_2S on the efficiency of plasma catalytic CH_4 and CO_2 conversion. Plasma and catalysis work well together, and this has been known for a long time. However, efforts to improve synergy and energy efficiency remain both highly desired and difficult because of the effect of poisoning the conversions of CO_2 and CH_4 and syngas ratio.

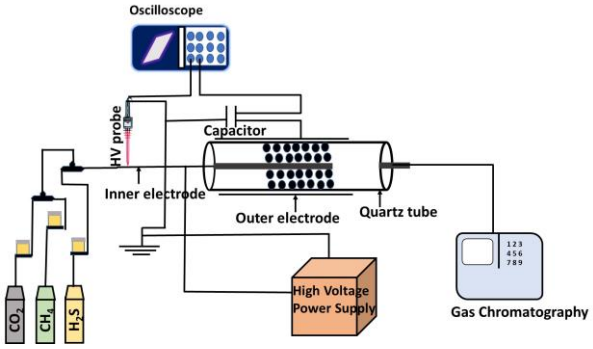

Fig. 1. Schematic diagram of experimental setup

2. EXPERIMENTAL

2.1 Experimental set-up

Fig. 1 illustrates the dielectric barrier discharge reactor employed in the process of biogas reforming. The flow rate was set to a constant value of 70 mL/min. A ground electrode is established by utilizing a quartz tube with an inner diameter of 20 mm, which is encased by a stainless-steel mesh. A high voltage electrode with a diameter of 11 mm is positioned at the center of the quartz tube to serve as the inner electrod e. The resulting discharge gap measures 4.5 mm. The discharge volume of the reactor is 24 cm^3 and was maintained for all the reactions. The dissipated power was determined using the Q-U Lissajous method. The experiment was initiated by conducting the reaction using CO_2, CH_4 and N_2 at flow rates of 30 mL min^{-1}, 30 mL min^{-1}, and 10 mL min^{-1} respectively. The reaction was carried out in a DBD reactor, both with plasma alone and in the presence of a catalyst. Following that, we repeated the experiment with a 10 mL/min flow of 0.054% H_2S diluted with N_2 injected into a mixture of CH_4 and CO_2, while keeping a constant residence time.

2.2 Gas analysis and parameter definitions:

The gas mixture from the reactor outlet was subjected to analysis using gas chromatography, equipped with a thermal conductivity detector by Mayura Analytical Pvt. Ltd. The elution of the gaseous molecules was performed using Molecular Sieve 5A and HayaSep-A columns. The parameters were derived using the following equations.

$$\mathrm{CO_2\ conversion\ (\%)} = \frac{\mathrm{converted\ CO_2\ (mmol/mL)}}{\mathrm{CO_2\ input\ (mmol/mL)}}\ \mathrm{X}\ 100$$

$$\mathrm{CH_4\ conversion\ (\%)} = \frac{\mathrm{converted\ CH_4\ (mmol/mL)}}{\mathrm{CH_4\ input\ (mmol/mL)}}\ \mathrm{X}\ 100$$

$$\text{CO selectivity (\%)} = \frac{\text{CO produced (mmol/mL)}}{[\text{CH}_4 \text{ converted} + \text{CO}_2 \text{ converted}](\text{mmol/mL})} \times 100$$

$$\frac{\text{H}_2}{\text{CO}} = \frac{\text{H}_2 \text{ produced (mmol/mL)}}{\text{CO produced (mmol/mL)}}$$

$$\text{H}_2 \text{ selectivity (\%)} = \frac{\text{H}_2 \text{ produced (mmol/mL)}}{2 \text{ X } \text{CH}_4 \text{ converted (mmol/mL)}} \text{ X } 100$$

$$\text{EE (mmol/kJ)} = \frac{[\text{CH}_4 \text{ converted} + \text{CO}_2 \text{ converted}]}{\text{Power (W)}} \text{X} \frac{1000}{60}$$

$$\text{CB (\%)} = \frac{[\text{CH}_4 \text{ output} + \text{CO}_2 \text{ output}] + \text{CO produced (mmol/mL)}}{[\text{CH}_4 \text{ input} + \text{CO}_2 \text{ input}](\text{mmol/mL})} \text{ X } 100$$

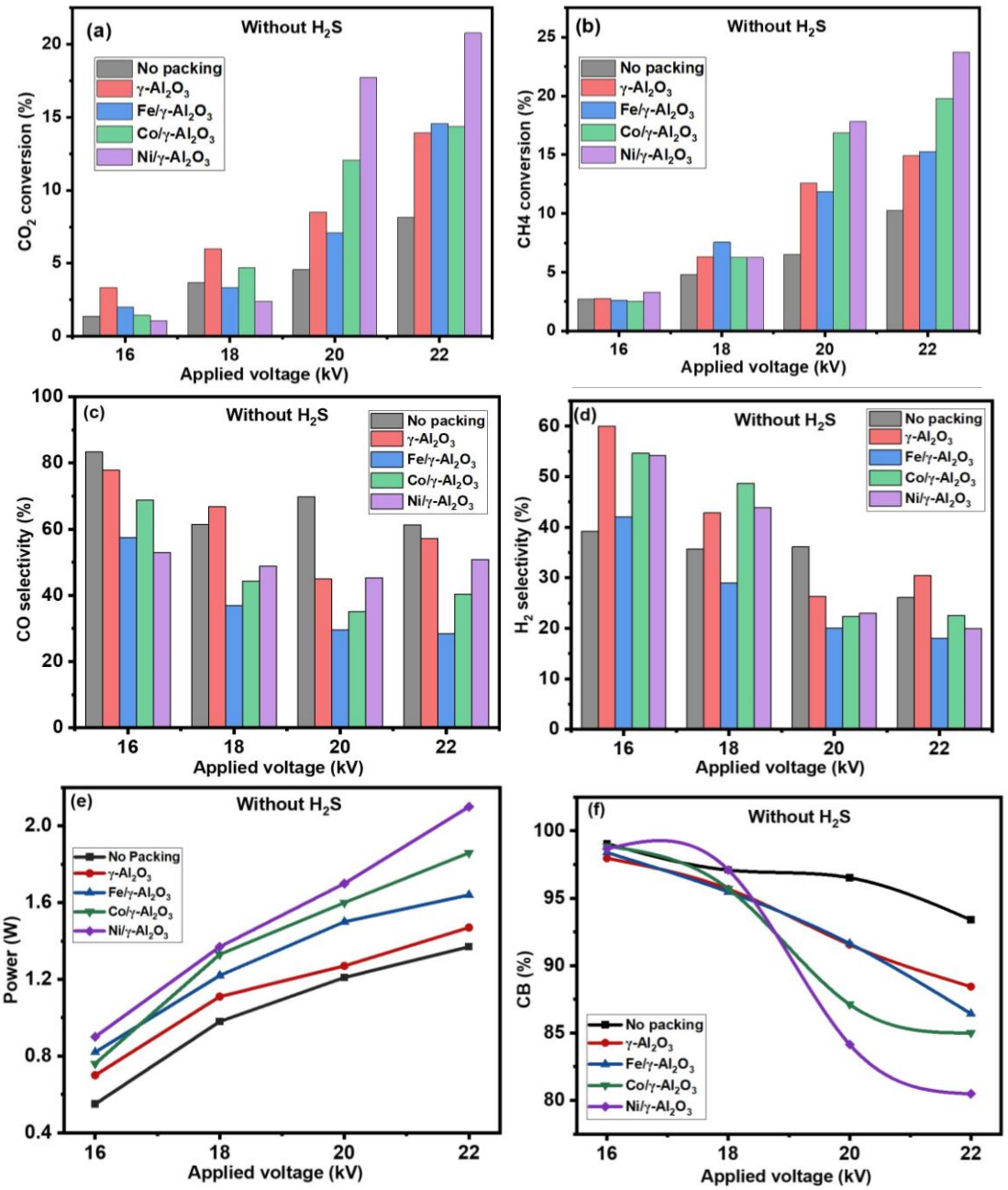

Fig. 2. (a) & (b) CO_2 and CH_4 conversion, (c) & (d) CO and H_2 selectivity, (e) & (f) power and carbon balance, plotted against applied voltage.

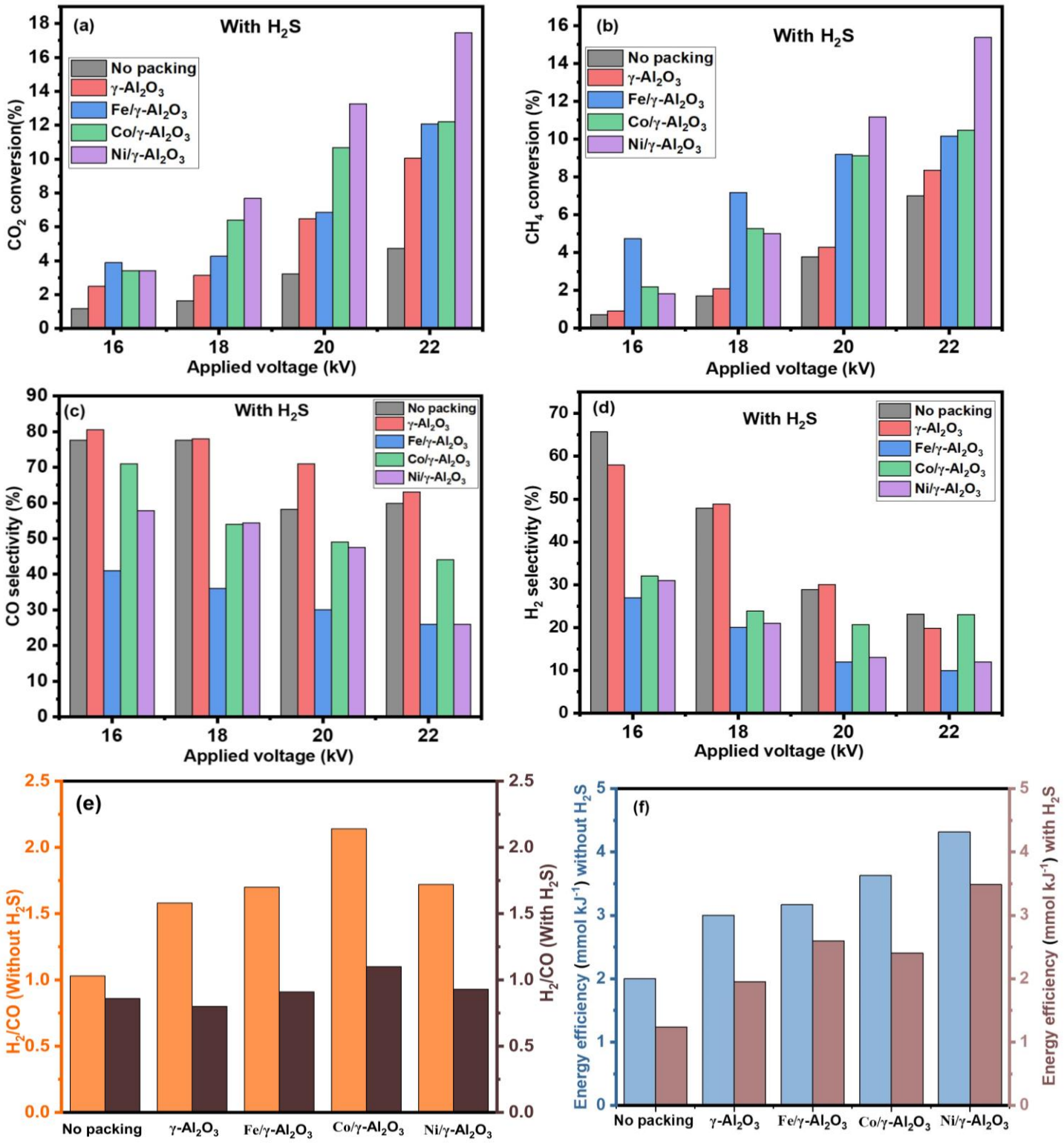

Fig 3. (a) & (b) CO_2 and CH_4 conversion, (c) & (d) CO and H_2 selectivity plotted against applied voltage. (e) & (f) H_2/CO ratio and energy efficiency with no packing and packed materials at an applied voltage of 22 kV.

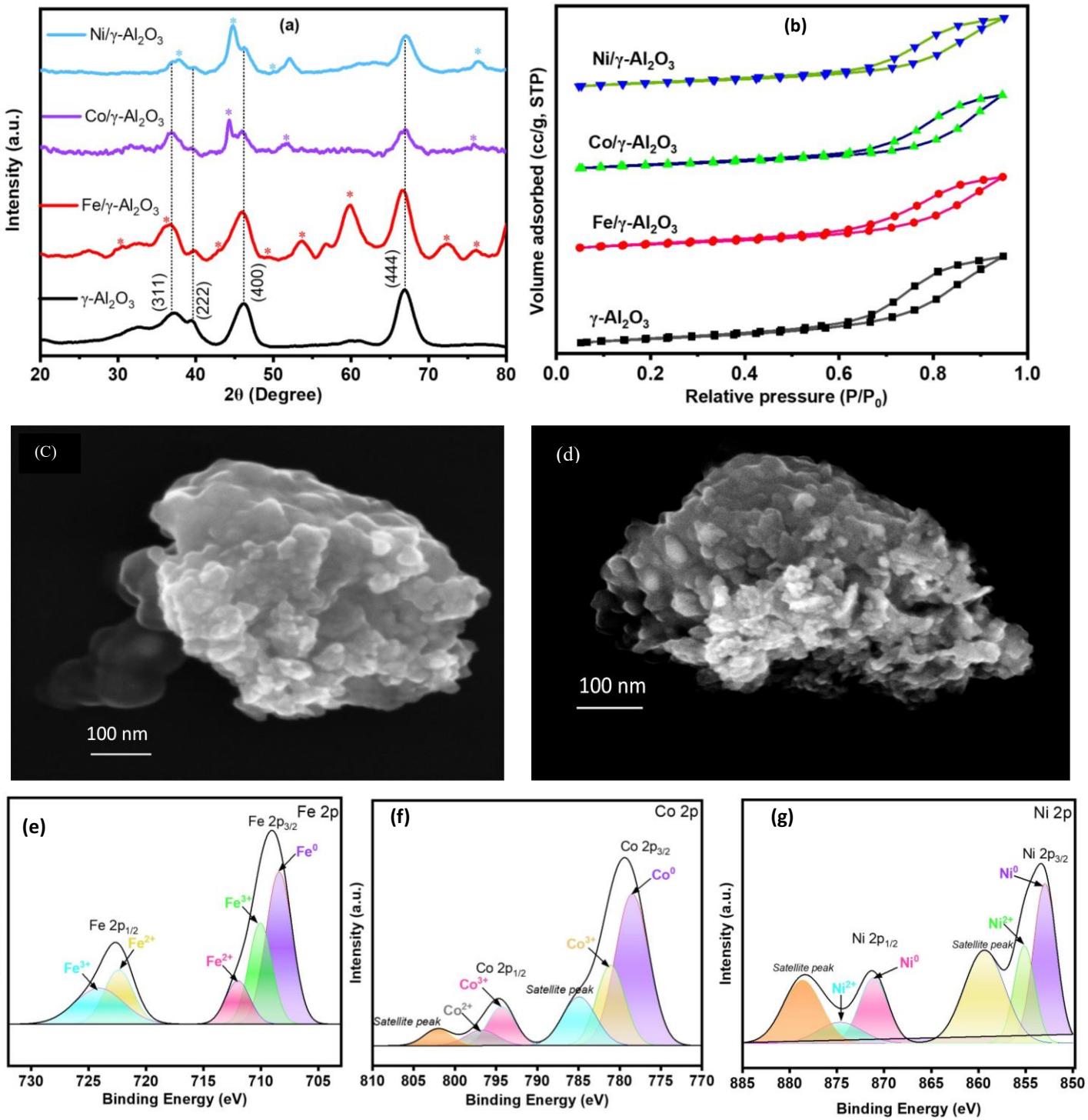

Fig. 4. (a) XRD spectra, (b) BET analysis of the prepared catalysts, (c) & (d) SEM images of Ni/γ-Al_2O_3 catalyst fresh and H_2S treated respectively. (e-g) XPS spectra of prepared catalyst.

3. MATERIAL AND METHODS

The catalysts were synthesized using an incipient wetness impregnation method. The metal precursor solutions were prepared by dissolving each metal salt $Ni(NO_3)_2{\cdot}6H_2O$) ($Co(NO_3)_2{\cdot}6H_2O$, and $Fe(NO_3)_3{\cdot}9H_2O$, in a small quantity of water that was precisely enough to occupy the void spaces of the γ-Al_2O_3 support. The γ-Al_2O_3 underwent an initial calcination process at a temperature of 400°C for a duration of 5 h to eliminate any impurities, such as adsorbed H_2O. Subsequently, it was introduced into the precursor solution and subjected to stirring until complete homogeneity was

achieved. The resultant mixture was maintained at ambient temperature for a duration of 3 h, followed by subsequent drying at a temperature of 80°C over the night. Subsequently, calcination was done at a temperature of 500°C for a duration of 4 h. Finally, all the prepared catalysts were reduced in a tubular furnace at 700°C with H_2 gas.

3.1 Catalyst characterization

The X-ray diffraction (XRD) patterns of the catalysts were acquired using Rigaku Pro XRD instrument equipped with Cu-K_α radiation source. The measurements were conducted within 2θ range of 20°–80°. The physisorption properties of the catalysts were assessed by conducting N_2 adsorption/desorption measurements on a NOVA2200e automated gas sorption analyzer (Quantachrome, USA) at a constant temperature of 77 K using liquid nitrogen. Before analysis, all samples were pre-treated, which involved degassing at 300°C for a duration of 3 h under a vacuum. Catalyst morphologies were characterized by using a scanning electron microscopy. X-ray photoelectron spectroscopy (XPS) was employed to identify the catalyst's surface chemical composition and oxidation state. The analysis was conducted using an AXIS Supra-Kratos analytical spectrophotometer equipped with a monochromatic X-ray source, specifically Al-K_α, with an energy of 1486.6 eV.

4. RESULTS

4.1 XRD and XPS analysis

X-ray diffraction analysis was conducted on the catalysts in their pristine state prior to initiating the reaction. Prominent peaks corresponding to γ-Al_2O_3 are observed in all XRD patterns, as depicted in **Fig. 4a**. The presence of these peaks is shown at 2θ = 36.9°, 39.7°, 46.2°, 66.98°, corresponding to the cubic structure of γ-Al_2O_3 crystalline (PDF# 10-0425). All these peaks can also be observed in the XRD patterns of the fresh M/γ-Al_2O_3 (M=Fe,Co,Ni) catalysts. Fe/γ-Al_2O_3 shows Fe_2O_3 phase at 2θ = 35.7°, 49.8°, and 54.4° in the spectra, and other peaks were also observed for metallic form of Fe.[15] XRD pattern of the Co/γ-Al_2O_3 catalyst shows the formation of Cobalt oxide originating from the decomposition of $Co(NO_3)_2$ into CoO and subsequent oxidation of the CoO species to Co_2O_3 which upon further reaction with CoO converted to Co_3O_4. The peaks of the two Co containing phases, Co_3O_4 and $CoAl_2O_4$ were difficult to distinguish due to a very slight difference in their lattice constants. These phases are also present in the prepared catalyst.[16] XRD pattern of the Ni/γ-Al_2O_3 shows the reduced metallic Ni from its oxide form at 2θ = 44.4°, 51.6°, and 76.08°. NiO is also present, but with less intensity.[17]

XPS result of the prepared catalysts is presented in **Fig. 4 (e-g).** The binding energies of the Fe 2p, Co 2p and Ni 2p are reported. The binding energies for the Fe $2p_{3/2}$ are around 708.4 eV, 710.8 eV and Fe $2p_{1/2}$, are around 722.5 eV and 724.4 eV in the Fe 2p spectra. Fig. 4e confirms the Fe^0, Fe^{3+} and Fe^{2+} for the Fe/γ-Al_2O_3 catalyst.[18,19] In the acquired Ni2p spectra (Fig. 4g), the peaks $Ni2p_{3/2}$ and $Ni2p_{1/2}$ can be observed. The most significant $Ni2p_{3/2}$ and $Ni2p_{1/2}$ peaks are found at binding energies of 852.9 eV and 871.1 eV for NiO and 855.1 eV and 874.6 eV for Ni^{2+} respectively.[20] The binding energies of Co $2p_{3/2}$ and its satellite peak were discovered at 779.0, 782.7 and 786.1 eV respectively, whereas those of $Co2p_{1/2}$ and its satellite peak were discovered at 794.4, 796.16, and 802.3 eV respectively.[21] These demonstrate the coexistence of CoO, Co^{2+} and Co^{3+} in the sample which is shown in Fig. 4f.

4.2 BET analysis

The observed variations in surface area among the catalysts (**Table 1**) were minimal and did not exhibit a consistent correlation with the achieved conversions in the biogas reforming reaction. **Fig. 4b** shows the BET isotherms. Consequently, the determination of reaction performance was not primarily influenced by the surface area and, consequently, the number of active sites present on the catalyst surface. All the catalysts, in fact, had a lower surface area than the alumina support because of the blockage of pores of γ-Al_2O_3 by the metal atoms. γ-Al_2O_3 is well-known for its high porosity and substantial surface area. Consequently, when the alumina bead is coated with a catalyst material of lower porosity, the surface area of the combined catalyst + alumina is decreased when compared with alumina alone. All catalysts have a Type-V isotherm and an H3-type hysteresis loop at relative pressures between 0.5 and 0.95, which suggests the existence of mesopores.

Table 1. BET analysis was used to evaluate the surface area, pore volume, and pore size of γ-Al_2O_3 and the other metal catalysts used in the plasma-catalytic biogas reforming reaction.

Catalyst	S_{BET} (m^2/g)	Total Pore volume (cm^3/g)	Average Pore size (nm)
γ-Al_2O_3	263	0.758	5.7
Fe/ γ-Al_2O_3	242	0.646	5.35
Co/ γ-Al_2O_3	213	0.614	5.76
Ni/ γ-Al_2O_3	208	0.573	5.3

4.3 Effect of catalysts on discharge characteristics

Fig. 5 shows the Q-V Lissajous figure employed in the estimation of power dissipation during plasma discharge. When transition metal catalysts are introduced into the discharge zone of the DBD reactor, area of the Lissajous figure increased comparison to a system without the catalyst. **Fig. 2e** shows that DBD packed with catalyst showed the highest power compared to no packed DBD, due to the greater occurrence of micro discharges and filamentary discharges within the plasma.[22,23] The commonly observed phenomenon is that the quantity of charge transfer during each half cycle reduces as the applied voltage decreases. This reduction in charge transfer can potentially decrease the generation of highly energetic electrons and active plasma species.
The discharge characteristics exhibit noticeable changes in the plasma reactor when catalyst packing is present and absent, as depicted in **Table 2**. Detailed calculation of plasma parameters procedure was provided in our recent article.[24] Despite using different catalytic materials, there was no notable change in the discharge parameters. The dielectric capacitance of the empty DBD is measured to be 0.81 µF, while the DBD plasma with Ni/ γ-Al_2O_3 exhibits a capacitance of 1.22 µF. Also, changes were observed with cell capacitance, charge transfer per half cycle, peak to peak charge transfer as well. Therefore, it can be deduced that the choice of packing material has an impact on the performance of the reaction.

Table 2. Influence of catalyst packing on the plasma discharge.

Plasma mode	Power (W)	Qpk-pk (µC)	dQ (µC)	C_d (µF)	C_{cell} (µF)
P only	1.35	10.9	6.3	0.81	0.19
P+γ-Al_2O_3	1.47	11.8	7.9	0.86	0.22
P+Fe/ γ-Al_2O_3	1.66	12	8.7	0.85	0.23
P+Co/ γ-Al_2O_3	1.86	12.3	8.4	0.94	0.27
P+Ni/ γ-Al_2O_3	2.1	12.5	8.8	1.22	0.23

*P=Plasma

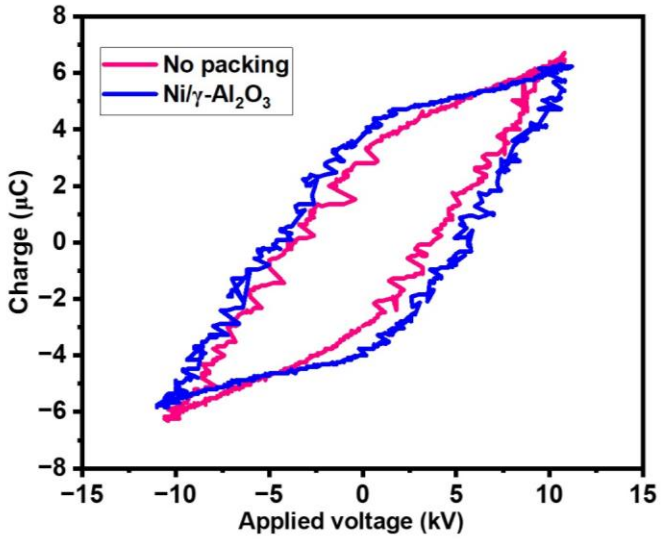

Fig. 5. Q-V Lissajous figures of the plasma alone and Ni/γ-Al_2O_3 packing with plasma.

4.4 Biogas conversion

The conversions of CO_2 and CH_4 were investigated in relation to the applied voltage, employing various transition metal catalysts which are shown in **Fig. 2 (a & b)**. In all instances, the conversions of gas exhibited an upward trend in correspondence with the escalation of applied voltage. In this study, the augmentation in applied voltage is attained through discharge power while maintaining a constant frequency. This procedure leads to the generation of additional reaction channels and intensifies the charge transfer in plasma chemical reactions. Consequently, the augmentation in discharge

power induces a corresponding escalation in the magnitude of micro discharges within the discharge gap, thereby enhancing the CO_2 and CH_4 conversion. In comparison to the plasma-only system, the integration of DBD with transition metal catalysts resulted in a marginal improvement in the conversion of biogas. The integration of Ni/γ-Al_2O_3 catalyst in discharge zone of the DBD reactor has been found to have the maximum CO_2 and CH_4 conversion compared to other catalysts.

4.5 Formation of main gas products

The major products CO and H_2 are produced during the biogas reforming reaction. **Fig. 2 (c & d)** depicts the selectivity of CO and H_2 with and without catalysts at various applied voltages. The distribution of products is primarily influenced by the catalyst packed DBD.

In all cases, it was observed that an increase in voltage resulted in a decrease in the selectivity of both carbon monoxide (CO) and hydrogen (H_2). This behavior may be attributed to Boudouard reaction in the discharge zone. The process of coke formation is observed to occur concurrently with the ongoing reaction. **Fig. 2f** shows the decrease in carbon balance with increased applied voltage. Within the discharge zone, solid carbon is deposited onto the inner surfaces of the quartz material, cylindrical quartz tube and the interface between the inner electrode and the tube. The limited specificity of H_2 gas can be attributed to the relatively less probable reverse water gas shift reaction. Furthermore, it is possible for the synthesis of higher hydrocarbons. However, the presence of these higher hydrocarbons was not detected in our gas chromatography due to analytical limitations. Xin Tu et al., reported that higher hydrocarbons also formed during the biogas reaction with DBD reactor.[25]

4.6 Influence of H_2S on Biogas reforming

After doing a biogas reforming experiment without H_2S, similar experiments were carried out with H_2S to examine its effect on the reaction when packed with different catalyst materials in the DBD reactor while conducting a biogas reforming experiment. In the context of biogas reforming using plasma catalysis, the rate of conversion of both CH_4 and CO_2 experienced a significant decrease in all the conditions upon the introduction of H_2S into the reaction mixture. SEM images confirm that the presence of localized aggregation of sulfur deposits on the catalysts surface decreases the catalytic activity. **Fig. 3 (a-d)** shows the conversion of gas and product gas selectivity in the presence of H_2S in the reaction mixture. DBD packed with Ni/γ-Al_2O_3 catalyst conversion rates dropped for CH_4 from 24% to 15%, and for CO_2 from 21% to 17%, in the absence and presence of H_2S, respectively. As shown in **Fig. 3(e)**, the H_2/CO ratio of the product gas in the packed DBD consistently exceeded that of the unpacked DBD, irrespective of the absence or presence of H_2S. A maximum syngas ratio of 2.14 was attained when employing Co/γ-Al_2O_3 used in a DBD reactor in the absence of H_2S. However, upon introducing H_2S into the gas mixture, the syngas ratio dropped from 2.14 to 1.1 with Co/γ-Al_2O_3 packed DBD, primarily due to the adverse impact of the poison effect.[9,26]

Fig. 3f demonstrates the calculation of energy efficiency at the highest discharge power in both an empty plasma reactor and a DBD packed with catalysts. The energy efficiency achieved using Ni/γ-Al_2O_3 is around 4.2 mmol/kJ. Across all scenarios, the packed DBD consistently exhibited maximum energy efficiency when compared to the unpacked DBD. Although there was only a slight difference in energy efficiency when using various catalyst materials, the introduction of H_2S into the reaction mixture caused a decrease in energy efficiency in all instances.

5. DISCUSSION

In the context of plasma catalysis, it is frequently noted that catalyst surfaces tend to display a higher degree of surface discharges, whereas streamer filaments are primarily limited to the empty spaces within the DBD reactor. This observation implies that surface reactions have the potential to exceed plasma gas-phase reactions in terms of their relevance and influence. To enhance comprehension of coke and sulfur deposition, SEM images were captured for both fresh catalysts and spent (with H_2S) catalyst of Ni/γ-Al_2O_3.These images were utilized to discern and analyze any discernible disparities on the catalytic surface. (**Fig. 4 c&d**). In **Fig.4d**, SEM image was obtained of a catalyst that had been subjected to a gas stream containing 0.054% H_2S. The image revealed the presence of localized aggregation of sulfur deposits on the catalyst's surface.

6. CONCLUSIONS

Our investigation involved examining the plasma catalytic conversion of biogas into syngas. The impact of H_2S on the conversions of CH_4 and CO_2 was investigated.

It was observed that the influence of 0.054 % H_2S resulted in a significant decrease in the conversions of CH_4 and CO_2 drastically decreased from 24% and 21% to 15% and 17%, respectively. Based on the examination of the catalyst's characteristics, it was found that the coke deposition and sulfur deposition that happened during the reaction on the catalyst's surface, which showed the efficiency of the reaction there was a significant level of dominance in the absence of H_2S, but this dominance decreased when H_2S was introduced. In contrast, it was observed that the reaction performance drastically changes during sulfur deposition under given conditions. Based on the results of this study, it can be inferred that neglecting the existence of H_2S in the process of biogas reforming is an incorrect assumption.

ACKNOWLEDGEMENT: M. Umamaheswara Rao expresses gratitude to the University Grants Commission of India for providing Senior Research Fellowship. The authors thank Indian Institute of Technology Hyderabad for providing the required research facilities.

DECLARATION OF INTEREST STATEMENT

The authors declare that they have no known competing financial interests or personal relationships that could have appeared to influence the work reported in this paper. All authors read and approved the final manuscript.

REFERENCE

[1] M.-S. Fan, A.Z. Abdullah, S. Bhatia, Catalytic Technology for Carbon Dioxide Reforming of Methane to Synthesis Gas, ChemCatChem. 1 2009;192–208.

[2] M. Zhumabek, G. Xanthopoulou, S.A. Tungatarova, T.S. Baizhumanova, G. Vekinis, D.Y. Murzin, Biogas Reforming over Al-Co Catalyst Prepared by Solution Combustion Synthesis Method, Catalysts. 11 2021;274.

[3] N. Abatzoglou, S. Boivin, A review of biogas purification processes, Biofuels Bioprod. Biorefining. 3 2009;42–71.

[4] M.U. Rao, D. Singh, K. Bhargavi, R.K. Sahu, S. Asthana, Ch. Subrahmanyam, Biogas reforming to syngas in a DBD plasma reactor with dielectric materials packing: Effect of H2S on the conversion of CH4 and CO2, Biomass Bioenergy 173 2023 106781.

[5] X. Tu, J.C. Whitehead, Plasma-catalytic dry reforming of methane in an atmospheric dielectric barrier discharge: Understanding the synergistic effect at low temperature, Appl. Catal. B Environ. 125 (2012) 439–448.

[6] A. George, B. Shen, M. Craven, Y. Wang, D. Kang, C. Wu, X. Tu, A Review of Non-Thermal Plasma Technology: A novel solution for CO2 conversion and utilization, Renew. Sustain. Energy Rev. 135 (2021) 109702.

[7] A. Bogaerts, T. Kozák, K. van Laer, R. Snoeckx, Plasma-based conversion of CO 2 : current status and future challenges, Faraday Discuss. 183 (2015) 217–232.

[8] A.H. Khoja, M. Tahir, N.A.S. Amin, Recent developments in non-thermal catalytic DBD plasma reactor for dry reforming of methane, Energy Convers. Manag. 183 (2019) 529–560.

[9] D. Mei, B. Ashford, Y.-L. He, X. Tu, Plasma-catalytic reforming of biogas over supported Ni catalysts in a dielectric barrier discharge reactor: Effect of catalyst supports, Plasma Process. Polym. 14 (2017) 1600076.

[10] M.-W. Li, Y.-L. Tian, G.-H. Xu, Characteristics of Carbon Dioxide Reforming of Methane via Alternating Current (AC) Corona Plasma Reactions, Energy Fuels. 21 (2007) 2335–2339.

[11] Z. Bo, J. Yan, X. Li, Y. Chi, K. Cen, Plasma assisted dry methane reforming using gliding arc gas discharge: Effect of feed gases proportion, Int. J. Hydrog. Energy. 33 (2008) 5545–5553.

[12] D.Y. Kalai, K. Stangeland, W.M. Tucho, Y. Jin, Z. Yu, Biogas reforming on hydrotalcite-derived Ni-Mg-Al catalysts: the effect of Ni loading and Ce promotion, J. CO2 Util. 33 (2019) 189–200.

[13] H. Wang, B. Zhao, L. Qin, Y. Wang, F. Yu, J. Han, Non-thermal plasma-enhanced dry reforming of methane and CO2 over Ce-promoted Ni/C catalysts, Mol. Catal. 485 (2020) 110821.

[14] A.F. Lucrédio, J.M. Assaf, E.M. Assaf, Reforming of a model biogas on Ni and Rh–Ni catalysts: Effect of adding La, Fuel Process. Technol. 102 (2012) 124–131.

[15] L. Zhou, L.R. Enakonda, Y. Saih, S. Loptain, D. Gary, P. Del-Gallo, J.-M. Basset, Catalytic Methane Decomposition over Fe-Al2O3, ChemSusChem. 9 (2016) 1243–1248.

[16] N.F. Khairudin, M. Mohammadi, A.R. Mohamed, An investigation on the relationship between physicochemical characteristics of alumina-supported cobalt catalyst and its performance in dry reforming of methane, Environ. Sci. Pollut. Res. 28 (2021).

[17] F. Zhu, H. Zhang, X. Yan, J. Yan, M. Ni, X. Li, X. Tu, Plasma-catalytic reforming of CO2-rich biogas over Ni/γ-Al2O3 catalysts in a rotating gliding arc reactor, Fuel. 199 (2017) 430–437.

[18] P. Phyu Mon, P. Phyu Cho, L. Chanadana, K.V. Ashok Kumar, S. Dobhal, T. Shashidhar, G. Madras, Ch. Subrahmanyam, Bio-waste assisted phase transformation of Fe3O4/carbon to nZVI/graphene composites and its application in reductive elimination of

Cr(VI) removal from aquifer, Sep. Purif. Technol. 306 (2023) 122632.
[19] Z. Hou, P. Yan, B. Sun, H. Elshekh, B. Yan, An excellent soft magnetic Fe/Fe3O4-FeSiAl composite with high permeability and low core loss, Results Phys. 14 (2019) 102498.
[20] P.P. Mon, P.P. Cho, L. Chandana, V.V.S.S. Srikanth, G. Madras, S. Ch, Biowaste-derived Ni/NiO decorated-2D biochar for adsorption of methyl orange, J. Environ. Manage. 344 (2023) 118418.
[21] L. Li, Q. Yuan, S. Ye, Y. Fu, X. Ren, Q. Zhang, J. Liu, In situ formed lithium ionic conductor thin film on the surface of high-crystal-layered LiCoO2 as a high-voltage cathode material, Mater. Chem. Front. 5 (2021) 6171–6181.
[22] M. Umamaheswara Rao, K.V.S.S. Bhargavi, P. Chawdhury, D. Ray, S.R.K. Vanjari, Ch. Subrahmanyam, Non-thermal plasma assisted CO2 conversion to CO: Influence of non-catalytic glass packing materials, Chem. Eng. Sci. 267 (2023) 118376..
[23] P. Chawdhury, D. Ray, T. Vinodkumar, Ch. Subrahmanyam, Catalytic DBD plasma approach for methane partial oxidation to methanol under ambient conditions, Catal. Today. 337 (2019) 117–125.
[24] M. Umamaheswara Rao, K. Bhargavi, G. Madras, Ch. Subrahmanyam, Basic metal oxide integrated DBD packed bed reactor for the decomposition of CO2, Chem. Eng. J. 468 (2023) 143671.
[25] Y. Zeng, G. Chen, J. Wang, R. Zhou, Y. Sun, A. Weidenkaff, B. Shen, X. Tu, Plasma-catalytic biogas reforming for hydrogen production over K-promoted Ni/Al2O3 catalysts: Effect of K-loading, J. Energy Inst. 104 (2022) 12–21.
[26] S.A. Chattanathan, S. Adhikari, M. McVey, O. Fasina, Hydrogen production from biogas reforming and the effect of H2S on CH4 conversion, Int. J. Hydrog. Energy. 39 (2014) 19905–19911.